Research Article
Open Access
Life Sciences, Medicine and Biomedicine

Anticancer combination effects of Doxorubicin and Curcumin on human breast cancer cell lines MDA-MB-231 and MCF-7

Yee Teng Wong, Ashley San Ann Soo, Ser Hui San and Siew Ching Ngai*

School of Biological and Environmental Sciences, Faculty of Science and Engineering, University of Nottingham Malaysia, 43500 Semenyih, Selangor.

Correspondence: Eunice.Ngai@nottingham.edu.my

Received 18 December 2024; Revised 28 December 2025; Accepted 16 January 2026; Published online 29 May 2026

ABSTRACT

Breast cancer remains one of the primary causes of death among women globally. Doxorubicin (DOX) is a widely used chemotherapeutic drug in breast cancer therapy. However, it is limited by the development of chemoresistance and its cardiotoxic effects. Curcumin (CUR), a natural anticancer agent is promising in promoting apoptosis in cancer cells while sparing the healthy cells. Therefore, this project aims to study the combined anticancer effects of DOX and CUR in the human breast cancer MDA-MB-231 and MCF-7 cells. The half inhibitory concentration (IC_{50}) of the combined DOX and CUR was determined prior to subjecting the cells treated with IC_{50} of the drugs to cell viability (MTT and trypan blue), wound healing, hematoxylin and eosin (H&E) staining and reverse transcription-polymerase chain reaction (RT-PCR) targeting *CDH1* by using *β-actin* as the housekeeping gene. The IC_{50} determined was 0.8 µM and 20 µM for DOX and CUR, respectively. The cell viability of MDA-MB-231 and MCF-7 decreased in time-dependent manner; however, MCF-7 exhibited a sudden increase at 48 hours, suggesting potential development of resistance. Trypan blue exclusion test showed that both cells displayed decreased cell viability, with MDA-MB-231 displayed greater decrease in cell viability. The cell migration of MDA-MB-231 was lower than the untreated cells at 72 hours while for MCF-7, the cell migration was reduced at 24 and 48 hours. H&E staining revealed various apoptotic morphological changes in the treated cells. RT-PCR results showed that *CDH1* expression was highest for MDA-MB-231 at 24 hours after the combined treatment, indicating reduced epithelial–mesenchymal transition (EMT), thus inhibited metastasis. In conclusion, the combined DOX and CUR treatment shows promising potential in enhancing the anticancer effects by reducing cell viability, inhibiting the cell migration pathway as well as inducing apoptosis execution, overall mitigating the limitations of the existing breast cancer therapies.

Keywords: *Breast cancer, anticancer, doxorubicin, curcumin and combined treatment*

INTRODUCTION

Cancer, a daunting word that takes 10 million lives every year. In the United States, breast cancer is the second prominent cause of cancer death in women, especially with 2.3 million women diagnosed in 2022 (World Health Organization, 2024). It is the reason why researchers all over the world are working hard to treat this leading cause of death worldwide.

Breast cancer is a malignant disease in which cells of the breast divide uncontrollably and form tumours due to a loss of apoptotic control (Yuan et al., 2022). Apoptosis is a natural occurring form of programmed cell death in most normal cells, but this process is often disrupted or evaded in cancer cells. The regulation of apoptosis is important for normal growth, development and homeostasis of cells. Dysregulation of normal apoptosis leads to the uncontrolled proliferation of cells and the eventual formation of a tumour. Therefore, the controlled regulation of apoptosis is critical in the treatment of cancer (Pilco-Ferreto & Calaf, 2016).

https://doi.org/10.28916/lsmb.10.1.2026.177

Additionally, contributing largely to its development and survival are cancer cell mechanisms to resist anticancer defences. These molecular mechanisms include chemoresistant expression of drug efflux pumps, where cancer cells increase expression of ATP-binding cassette (ABC) transporters. An example is multidrug resistance protein 1 (MDR1), which helps combat the cytotoxic effects. Changes in tissue architecture also exacerbate cancer invasion and development, where epithelial cells change towards mesenchymal phenotypes, characterised by a loss of E-cadherin (*CDH1*), thus losing cell adhesion and tissue organization properties and in turn, induction of cell motility facilitating cancer cell migration and metastasis (Feitelson et al., 2015).

With some success, established current strategies against the fight of breast cancer are radiotherapy, targeted therapy, chemotherapy, and surgical resection which serve as hopeful solutions. However, due to the neoplasm and heterogeneity of cancer genetics, new aggressive versions are on the rise, side effects such as relapse or drug resistance and risk to surrounding healthy tissues and organs, deem the current therapies insufficient, thus a better solution is imperative. With new drug discovery, early detection programmes, medical therapies, and increased interest towards breast cancer research, it only raises hope to those affected but a more efficient solution is still essential (Iacopetta et al., 2023).

MDA-MB-231 cells, an aggressive breast cancer cell line, serve as a widely used model for triple-negative breast cancer (TNBC) as they lack the expression of estrogen receptor (ER), progesterone receptor (PR) and human epidermal growth factor receptor 2 (HER2), rendering them unresponsive to receptor-targeted therapies. TNBC is notorious for a high death risk, recurrence, and metastasis, where there are no targeted therapy options, thus an effective treatment is still necessary (Chen et al., 2013). On the other hand, the MCF-7 cells are less aggressive luminal A breast cancer cells which are positive for ER and PR, thus respond better to targeted hormone-responsive cancer therapies.

DOX is a widely utilised cytotoxic chemotherapeutic drug, belonging to class I anthracyclines. With a 35% response rate to metastatic breast cancer, proving to be an effective chemotherapeutic drug, it is often also used for the treatment of prostate, lung, and ovarian malignancies, establishing itself as a diverse therapeutic option. This cytotoxic drug inhibits the topoisomerase II enzyme progression by intercalating between base pairs in the DNA helix, thus preventing proliferation and division of cancer cells, inhibiting DNA replication and thus resealing. It also increases reactive oxygen species generation, thus leading to a series of eventual cell death (Saharkhiz et al., 2023). However, although effective, its life-threatening side effects such as multidrug resistance development, potential acute toxicity to non-target healthy cells due to lack of specificity and cumulative cardiotoxicity, render it an incomplete solution (Lee et al., 2023). Its short half-life and immunogenicity emphasise the room for improvement. Therefore, to combat these harmful side effects and conserve its usefulness, a combination of complementary anticancer drugs which can increase the therapy sensitivity is warranted.

CUR is a natural bioactive product sourced and isolated from the rhizome of *Curcuma longa*, often termed as turmeric. It has unique anti-inflammatory and potent antioxidant properties that serve as a prospective treatment against viral infections, arthritis, inflammatory skin and most importantly, cancer (Pulido-Moran et al., 2016). Many compelling studies have advocated CUR's ability to disrupt the cell proliferation and migration of cancer, where it has been studied to combat the chronic proliferation property of cancer through disrupting and blocking the activation of PI3K/Akt signalling pathway, that hugely responsible for the proliferation and metastasis of cancerous cells. Additionally, it has been studied to suppress NF-κB activation, thereby reducing tumour-promoting inflammation and survival signalling by downregulating pro-inflammatory cytokines and anti-apoptotic proteins (Xia et al., 2014; San & Ngai, 2025). In addition, CUR has been found to downregulate cyclin D1, a proto-oncogene that is frequently overexpressed in various cancers, ultimately contributing to cell cycle arrest (San & Ngai, 2025). CUR also proves to inhibit cell motility and metastasis through downregulating matrix metalloproteinases (MMPs), thus inhibiting EMT (Kewitz et al., 2013). Therefore, it is a promising anticancer solution that suppresses cell proliferation, cell cycle, invasion and migration as well as activating cell apoptotic pathways and inhibiting cancer hallmarks including tumour growth, inflammatory mediators and growth factors (Song et al., 2019). It being a natural product omits the risk of inducing adverse effects with similar therapeutic potential as its riskier counterparts. However, it has limited clinical efficacy due to its low bioavailability and water solubility (Klippstein et al., 2016).

With many clinical studies, complementary natural products, such as CUR, combined with a standard commercial cytotoxic drug such as DOX, can increase efficacy in anticancer effects (Saharkhiz et al., 2023). The combination of these anticancer agents can enhance inhibition of tumour growth and control its fatal progression (Jalaladdiny et al., 2022). Additionally, the natural anti-inflammatory and antioxidant properties of CUR aid in reducing the dose-limiting toxicity and adverse effects of DOX, proving to be a promising new solution (Sadzuka et al., 2012).

By aiming to enhance the effectiveness of chemotherapeutic agents and mitigate the issue of chemoresistance in cancer cells and dose limitation in patients, this study intends to assess the efficacy of the combined usage of DOX and CUR as a therapeutic treatment. The efficacy of the combined treatment will be evaluated by examining its impacts on cell viability, migration, and apoptosis in the TNBC cell line MDA-MB-231, with a focus on the EMT marker *CDH1*, with luminal A subtype MCF-7 cell line serving as a control. To date, no studies have reported the effects of combined DOX and CUR on *CDH1* expression, underscoring the novelty of this research.

MATERIALS AND METHODS

Chemicals

The analytical standard Curcumin (CUR) and Doxorubicin (DOX) were obtained from Sigma-Aldrich with purity by HPLC ≥ 98.0%, where CUR was dissolved in absolute ethanol and further diluted with Dulbecco's Modified Eagle Medium (DMEM) and DOX was dissolved in dimethyl sulfoxide (DMSO). Additionally, 3-(4,5-dimethylthiazol-2-yl)-2,5-diphenyltetrazolium bromide (MTT) (Sigma LifeScience, USA), trypsin-EDTA, phosphate-buffered saline (PBS), RNA extraction kit (Vivantis), RT-PCR kit (Vivantis), RT-PCR components (BIOLINE), 2% agarose gel and SyBr Safe were utilised. MTT was dissolved and diluted using 1X PBS.

Cell culture and maintenance

In this research, two human breast cancer cell lines (MDA-MB-231 and MCF-7 cells) were obtained from the Tissue Culture Laboratory, University of Nottingham Malaysia, which were originally purchased from American Type Culture Collection (ATCC). The cells were cultured and maintained in DMEM with 10% FBS (v/v) and 1% penicillin/streptomycin (v/v) (Jin et al., 2017; Lovitt et al., 2018), with a humidified atmosphere (with 5% CO_2) at 37°C. (Sheikholeslami et al., 2017).

Determination of DOX and CUR's combined IC_{50}

The half-maximal inhibitory concentration (IC_{50}) for the combined DOX and CUR on both breast cancer cell lines MDA-MB-231 and MCF-7 was determined using MTT assays. The cells were seeded at 5 x 10^3 cells per well in 96-well plates and incubated overnight. On the following day, the cells were treated with 0.2 µM of DOX and 5 µM of CUR, 0.4 µM of DOX and 10 µM of CUR, 0.6 µM of DOX and 15 µM of CUR, 0.8 µM of DOX and 20 µM of CUR. These concentrations were selected based on our previous study, which determined the IC_{50} values for DOX and CUR on MDA-MB-231 to be 0.8 µM and 20 µM, respectively (Kong et al., 2019, supplementary data), which tested DOX concentrations ranging from 0 to 1 µM and CUR concentrations from 0 to 50 µM.

After 24 hours of drug treatment, the culture medium was removed and 100 µL of MTT solution (1 mg/mL) was added (Wong et al., 2021). The cells were incubated for 4 hours at 37 ℃. Following 4 hours of incubation, the MTT solution was discarded, and 100 µL of DMSO was added to dissolve the purple formazan crystals formed. The net absorbance values were determined with a 96-well plate reader and was then calculated via subtraction of A_{630} from $A_{570.}$ (Wong et al., 2021). Cell viability of the treated cells was calculated using the formula: Cell viability = ($OD_{570\ nm - 630\ nm}$ of the treated cells / $OD_{570\ nm - 630\ nm}$ of the untreated cells) x 100%. The half maximal Inhibitory Concentration (IC_{50}) of DOX and CUR was determined as the drug concentration at which cell viability was reduced to approximately 50%.

Morphological observation of cells

MDA-MB-231 and MCF-7 cells were plated in 6-well plates at a density of 3 x 10^6 cells per well and incubated for 24 hours. After attachment, cells were exposed to the IC_{50} concentration of the combined treatment of DOX and CUR. After 24, 48 and 72 hours, the morphology of the cells was observed by using an inverted brightfield light microscope (Roudsari et al., 2012).

Cell viability assay

MDA-MB-231 and MCF-7 cells were plated in 96-well plates at a density of 5 x 10^3 cells per well and incubated. After attachment, cells were exposed to the IC_{50} concentration of DOX and CUR for 24, 48 and 72 hours. At the indicated timepoints, the cells were subjected to MTT assay, as described above. The cell viability of each sample was determined using the formula: Cell Viability = ($OD_{570nm-630nm}$ of treated cells/ $OD_{570nm-630nm}$ of untreated cells) × 100% (Yap et al., 2022).

Trypan blue exclusion test

Cell viability was further validated using the trypan blue exclusion assay. MDA-MB-231 and MCF-7 cells were seeded at 3 x 10^6 cells per well in 6-well plates and incubated overnight to allow attachment. The following day, the cells were treated with IC_{50} concentrations of DOX and CUR and incubated at 37˚C in a 5% CO_2 atmosphere for 24, 48 and 72 hours. At each time point, the culture medium was collected and centrifuged at 1500 rpm; the supernatant was then discarded. The cells in the 6-well plates were trypsinized with 1 ml of trypsin and allowed to incubate for 5 minutes. Following deactivation with basal media, cells were centrifuged at 1500 rpm and the supernatant was discarded. The resulting cell pellet was resuspended in 1 ml of DMEM. An equal volume of 0.4% trypan blue was mixed with the cell suspension at a 1:1 ratio. The cells were resuspended. The number of viable (unstained) and nonviable (stained) cells was counted

using a hemocytometer. The percentage of viable cells was calculated (Strober, 2015).

Wound healing assay

Cancer cell migration is one of the key processes driving cancer progression and metastasis. Drugs that inhibit cell migration have the potential to reduce metastatic spread, which is a major course of cancer-related mortality. Cell migration was assessed using a wound healing assay. MDA-MB-231 and MCF-7 cells were seeded at a density of 1×10^5 cells per well in 6-well plates and incubated overnight to allow attachment. By the following day, the cells formed a monolayer, where the plates were marked to be used as reference points as images were acquired before and after the assay for quantitative analysis. A wound was created by manually scraping the cell monolayer using a p200 pipette tip, applying consistent pressure and maintaining a uniform tip angle, where the wound was made perpendicular to the reference point on the well. The wound was then rinsed with PBS to withdraw any floating cells. The combined IC_{50} of DOX and CUR was added to the wells. The first image was then acquired before allowing incubation of the plates, where subsequent images were captured at the 24, 48 and 72 hours post treatment of DOX and CUR. After treatment, the wound closure was analysed using an inverted brightfield light microscope. The software ImageJ was then used with a standard size criterion where the distance of wound edges was quantified. Cell migration was determined by the difference in distance at 0 hours and distance at the specified timepoint divided by the distance at 0 hours (Rodriguez et al., 2005). The results are quantified through calculating the percentage of wound closure based on the cellular invasiveness of the resulting images (Wong et al., 2021).

Hematoxylin and eosin (H&E) staining

Histological H&E staining was performed to evaluate morphological changes in cells following combined treatment with DOX and CUR, in order to observe apoptotic morphologies of the cells. The cells were seeded at a density of 3 x 10^6 cells per well on coverslips in 6-well plates and incubated overnight. They were then treated with the IC_{50} concentration of DOX and CUR for 24, 48 and 72 hours. After treatment, the cells were fixed and rehydrated through descending concentrations of ethanol solutions (100% thrice, 95% twice and 70% once), for 3 minutes each time. The coverslips were then immersed in purified water for 5 minutes after rehydration. The rehydrated cells were then stained with hematoxylin for 5 minutes. The coverslips were then briefly dipped in diluted HCl for 2 seconds. The coverslips were then immersed in Scott's tap water for 5 minutes and then stained with eosin for 5 minutes. The cells were then dehydrated in increasing concentrations of ethanol solution for 3 minutes each time, firstly in 70% ethanol solution, then 95% of ethanol twice, then lastly 100% of ethanol twice. Then, the coverslips were immersed in xylene solution twice, each time for 5 minutes. The coverslips were then allowed to dry and mounted using permount solution (Sigma, USA). The stained cells were then examined under a light microscope (Lim et al., 2011). The images of the cells at different magnification were captured and analyzed. Cell morphology was observed to assess the efficacy of DOX and CUR in inducing apoptosis.

RT-PCR for the related gene *CDH1*

The cells were plated in 6-well plates and subsequently treated with IC_{50} concentration of DOX and CUR. After 24 hours of the treatment, the total RNA of the both breast cancer cells were extracted from cell pellets following the manufacturer's RNA extraction kit instructions (Vivantis) and reverse-transcribed into cDNA. RT-PCR was conducted using a two-step RT-PCR kit (Vivantis) where the related gene, *CDH1* was targeted alongside the housekeeping gene*, β-actin* (Sheikholeslami et al., 2017). The candidate genes' primer sequences are represented in Table 1.

PCR was performed under the following conditions: initial denaturation at 95°C for 5 minutes, followed by 30 cycles of denaturation at 95°C for 30 seconds, annealing at 54°C for *CDH1* and 55°C for *β-actin* for 30 seconds and extension at 72°C for 45 seconds. A final extension was carried out at 72°C for 5 minutes. PCR products were then subjected to electrophoresis on a 2% agarose gel stained with SyBr Safe (Wong et al., 2021). Expression level of *CDH1* was determined by measuring band intensities using ImageJ, normalized to *β-actin*, with the control set to 1 and treated samples expressed relative to the control.

Statistical analysis

Data are presented as mean ± Standard Error of the Mean (SEM) from triplicates across two independent experiments, unless otherwise stated. Statistical analysis was performed using IBM SPSS Statistics. ANOVA followed by Tukey *post-hoc* test was applied to determine statistical differences between treated and untreated samples.

Table 1

Details of primer sequences for the selected genes.

Primer Name	Primer sequence	
	Forward sequence	**Reverse sequence**
CDH1	5' - TTGACGCCGAGAGCTACAC - 3'	5'- GACCGGTGCAATCTTCAAA - 3'
β-actin	5'- AGAGCTACGAGCTGCCTGAC - 3'	5'- AGCACTGTGTTGGCGTACAG - 3'

Note: CDH1: E-cadherin gene; β-actin: Beta-globin gene

RESULTS

MTT assay for IC_{50} determination

MTT cell viability assay was performed to deduce the IC_{50} for the combined DOX and CUR. MTT assay was performed 24 hours post-treatment with DOX and CUR. The cell viability of MDA-MB-231 cells experienced reduction in a concentration-dependent manner. The cell viability of the untreated control was set at 100%. The cell viability decreased from 83% to 81%, 69% and 54% for the cells treated with increased concentrations of combined DOX and CUR from 0.2 µM DOX + 5 µM CUR to 0.4 µM DOX + 10 µM CUR, 0.6 µM DOX + 15 µM CUR and 0.8 µM DOX + 20 µM CUR. The IC_{50} concentration of the drug combination was defined as the concentration that reduced cell viability to approximately 50%. For the combined treatment, the IC_{50} values were determined to be 0.8 µM for DOX and 20 µM for CUR (Figure 1a).

MCF-7 cells incubated with increasing dosages of DOX and CUR show decreased cell viability, up until cells were treated with 0.8 µM of DOX and 20 µM of CUR. This trend is maintained for both independent experiments. The cell viability of the untreated control was set at 100%. The cell viability decreased from 95% to 82% and 78% as the concentrations of the combined treatment increased from 0.2 µM DOX+ 5 µM CUR to 0.4 µM DOX+ 10 µM CUR and 0.6 µM DOX + 15 µM CUR. However, the cell viability increased to 88% at the highest concentration of drugs (0.8 µM DOX+ 20 µM CUR) (Figure 1b).

Since the MDA-MB-231 is the TNBC, which is the target cell line is our study and the IC_{50} for the combined treatment is 0.8 µM of DOX and 20 µM of CUR. Therefore, these concentrations were used for the following experiments.

Figure 1

Percentage cell viability of MDA-MB-231 and MCF-7 treated with Doxorubicin (DOX) and Curcumin (CUR) after 24 hours post-treatment.

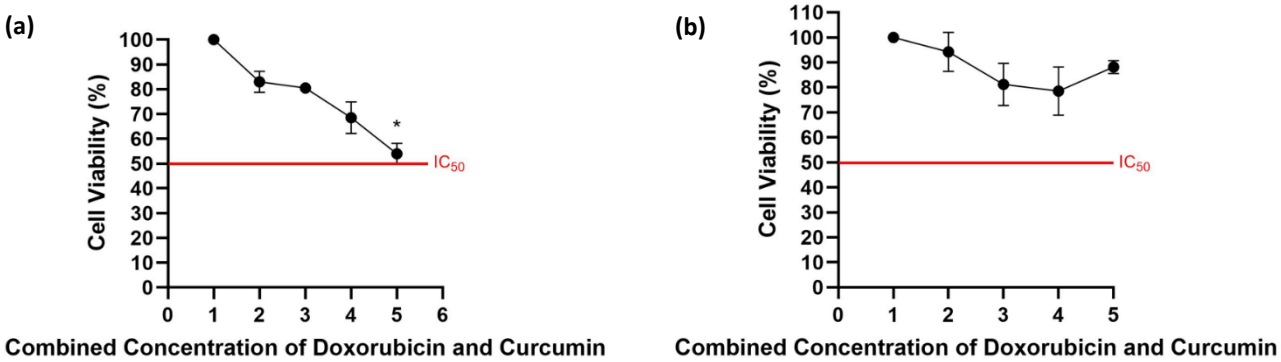

*Note: (a) MDA-MB-231. (b) MCF-7. The data represent mean ± SEM of triplicates from two independent experiments. *(p<0.05) represents significant differences from the untreated control. **1**: 0 µM DOX + 0 µM CUR; **2**: 0.2 µM DOX + 5 µM CUR; **3**: 0.4 µM DOX + 10 µM CUR; **4**: 0.6 µM DOX + 15 µM CUR; **5**: 0.8 µM DOX + 20 µM CUR.*

Morphological observation of cells

MDA-MB-231 and MCF-7 cells were grown in 6-well plates, wherein cells were treated with the IC_{50} concentration of DOX and CUR, while control cells were treated with only basal media (DMEM). In the control wells, cells were found to maintain their normal morphologies. Cells were found to grow and attach to the well surfaces. In cells treated with a combination of DOX and CUR, many floating cells were observed. Such cells were observed to be rounded in shape,

not displaying normal morphologies and were detached from the surface of the wells (Figures 2 and 3). Such morphologies and lack of adherent cells indicate apoptosis due to treatment from DOX and CUR. The decrease of cell density in a time-dependent manner suggests high rates of cell death.

Figure 2

Morphological observations of MDA-MB-231 cells post-treatment with IC_{50} of DOX and CUR at 24, 48 and 72 hours, respectively.

Note: The arrows highlight the floating, rounded cells that deviate from their typical morphology. The images were captured at 100x magnification.

Figure 3

Morphological observations of MCF-7 cells post-treatment with IC_{50} of DOX and CUR at 24, 48 and 72 hours, respectively.

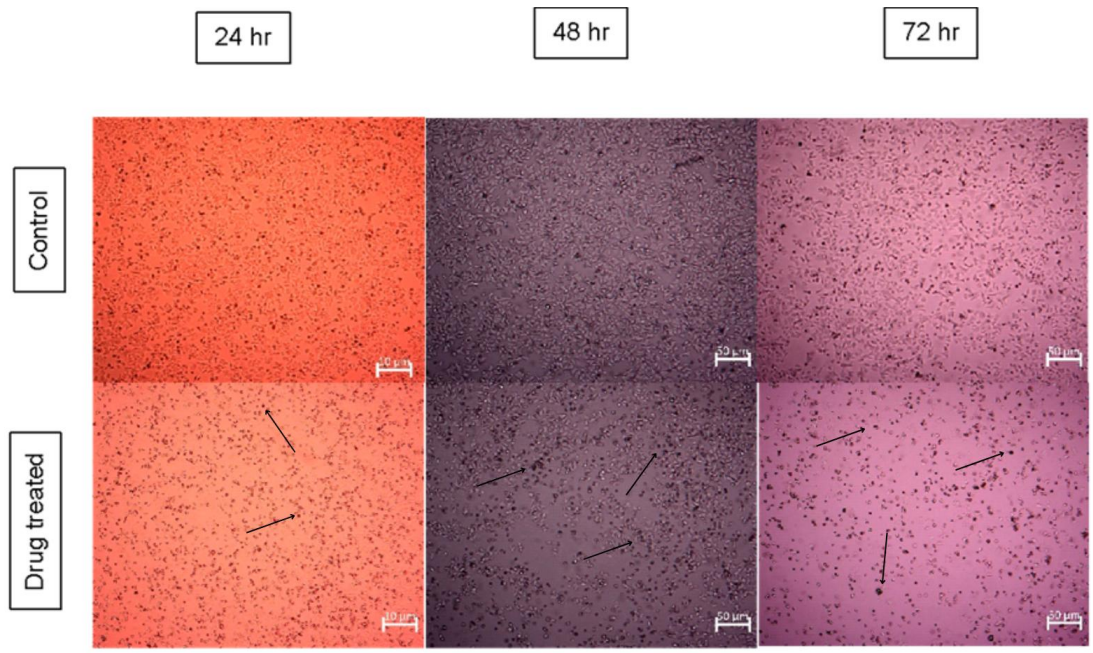

Note: The arrows highlight the floating, rounded cells that deviate from their typical morphology. The images were captured at 100x magnification.

Cell viability assay

The cytotoxic effect of combined treatment of DOX and CUR on MDA-MB-231 and MCF-7 cells at 24, 48 and 72 hours was evaluated using MTT cell viability assay. This combination treatment caused the viability of MDA-MB-231 cells to steadily decrease in a time-dependent manner, ultimately to 23%. Whilst for MCF-7 cells, it followed a trend of decreasing, however, the cell viability increased, and the cells proliferated immensely to 142% cell viability after 48 hours post treatment before returning to the expected trend of reducing viability, to 63% (Figure 4).

Trypan blue test of exclusion

Trypan blue exclusion assay revealed a marked reduction in cell viability in MDA-MB-231 cells following treatment. Viability at 24, 48 and 72 hours was 41.73%, 38.89% and 40.35%, respectively (Figure 5). In contrast, MCF-7 cells exhibited a more gradual, time-dependent decline in viability with values of 69.7%, 57.37% and 38.93% at 24, 48 and hours, respectively.

Figure 4

Percentage cell viability of MDA-MB-231 and MCF-7 cells determined by MTT assay at 24-, 48- and 72-hours post-treatment with IC_{50} of DOX and CUR.

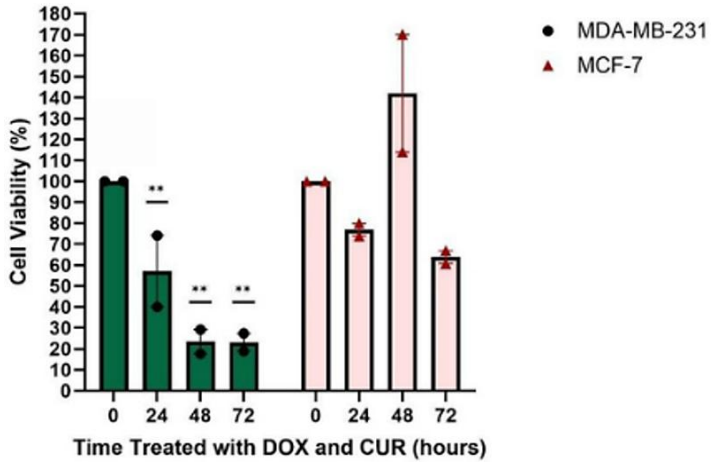

*Note: The error bars represent mean ± SEM of triplicates from two independent experiments. The significant difference between the control and treatment groups were reported as **, indicating significance (p < 0.001).*

Figure 5

Percentage of cell viability of MDA-MB-231 and MCF-7 cells determined by trypan blue exclusion test at 24-, 48- and 72-hours post-treatment with IC50 of DOX and CUR

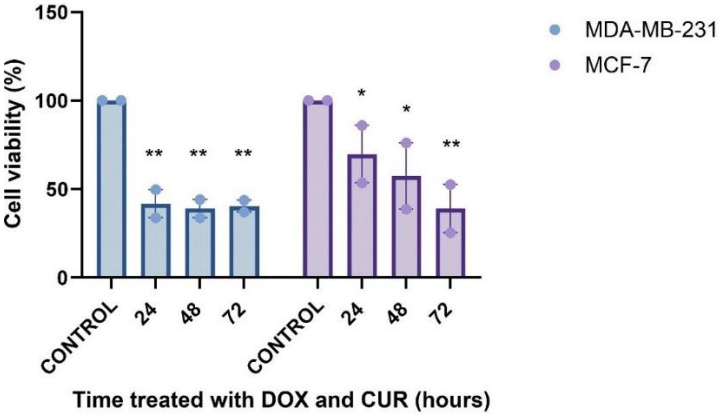

*Note: The error bars represent mean ± SEM of triplicates from two independent experiments. The significant difference between the control and treatment groups were reported as * and **, indicating significant (p<0.05) and very significance (p<0.001), respectively.*

Wound healing assay

As shown in Figure 6, MDA-MB-231 cells exhibited increased migration, indicated by a higher percentage of relative wound closure up to 48 hours post-treatment. At 72 hours post-treatment, the treated cells demonstrated a slight decrease in migration compared to untreated cells, with relative wound closure reducing from 104% to 99%. However, this reduction was not statistically significant (Figure 7).

For MCF-7 cells, as shown in Figures 8 and 9, no significant inhibition of cell migration was observed following treatment. The percentage of wound closure decreased from 100% to 94% and subsequently 82% at the 48 hours post-treatment compared to untreated cells. However, this trend was not sustained, as the relative wound closure increased at the 72 hours post-treatment, and this change remained statistically insignificant

Figure 6

Wound healing assay representative of MDA-MB-231 untreated and treated cells at 0, 24, 48 and 72 hours post-treatment with IC_{50} of DOX and CUR.

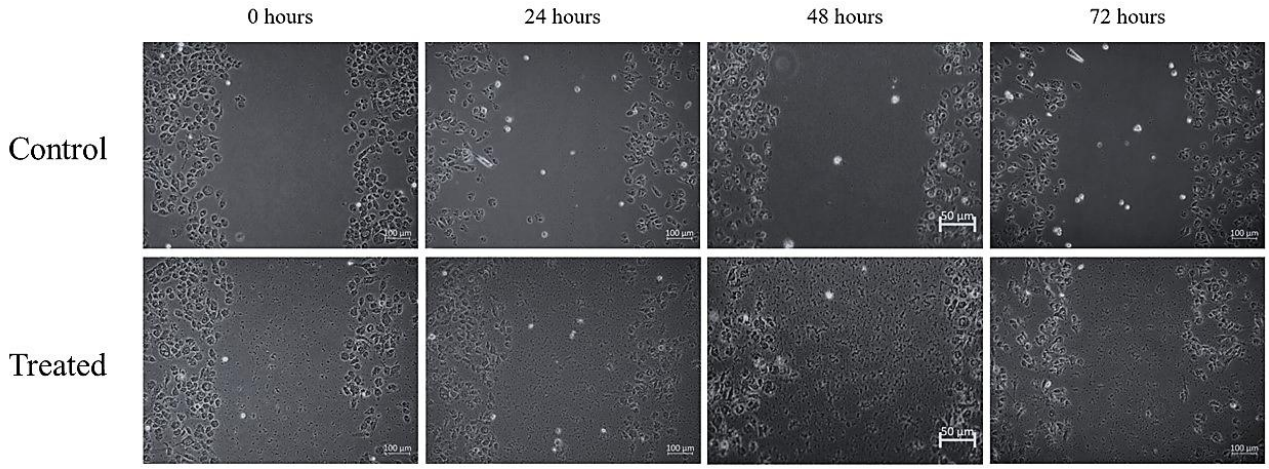

Note: The images were captured at 200x magnification.

Figure 7

Percentage relative wound closure of MDA-MB-231 cells at 0-, 24-, 48- and 72-hours post-treatment with with IC_{50} of DOX and CUR.

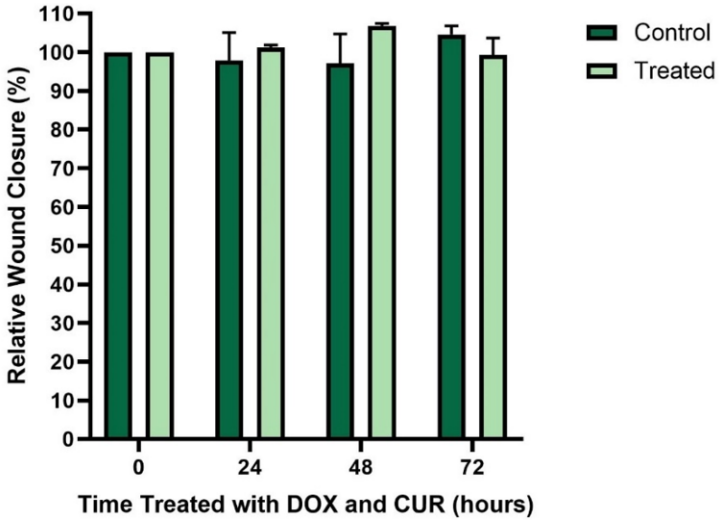

Note: The data represent mean ± SEM of triplicates from two independent experiments.

Figure 8

Wound healing assay representative of MCF-7 untreated and treated cells at 0, 24, 48 and 72 hours post-treatment with IC_{50} of DOX and CUR.

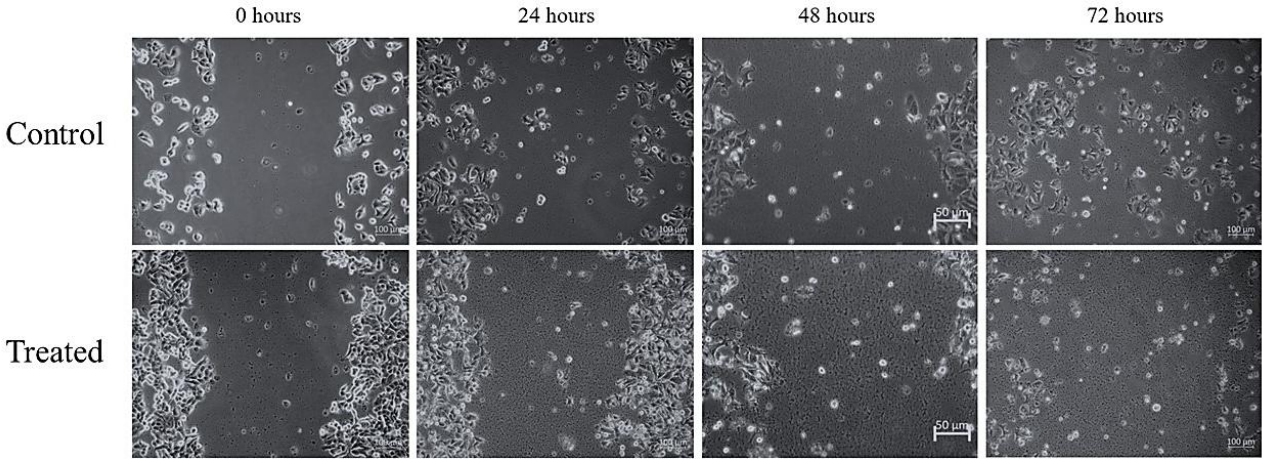

Note: The images were captured at 200x magnification.

Figure 9

Percentage relative wound closure of MCF cells at 0-, 24-, 48- and 72-hours post-treatment with IC_{50} of DOX and CUR.

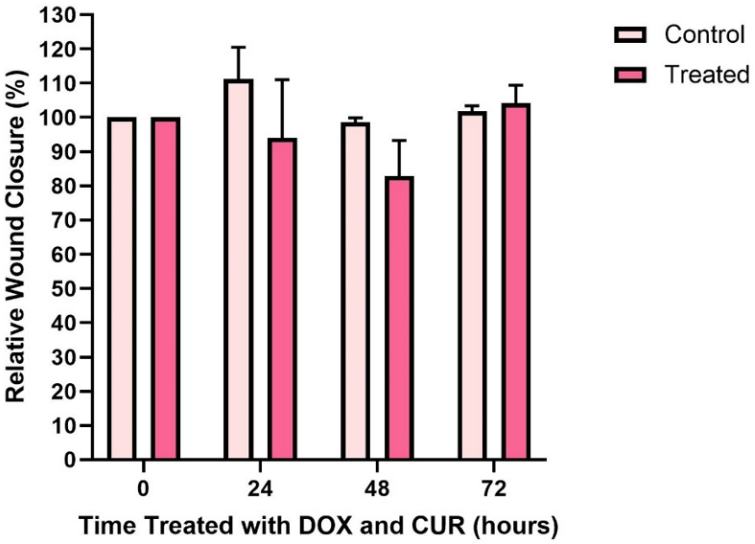

Note: The data represent mean ± SEM of triplicates from two independent experiments.

Hematoxylin and eosin (H&E) staining

Histological staining of MDA-MB-231 and MCF-7 cells was performed using H&E staining. The cells were observed for morphological changes indicative of apoptosis. Treated cells of both cell lines exhibited a considerable number of apoptotic morphologies after 24, 48 and 72 hours of treatment with DOX and CUR. Apoptotic features such as cell shrinkage, formation of apoptotic bodies, nuclear chromatin condensation and membrane blebbing were observed in MDA-MB-231 cells (Figure 10). Furthermore, obvious apoptotic features such as cytoplasmic shrinkage, membrane blebbing, cytoplasmic extension and the formation of apoptotic bodies were observed in MCF-7 cells post-treatment (Figure 11).

Figure 10

Hematoxylin and eosin (H&E staining) of MDA-MB-231 control cells (top row) and treated cells (bottom row) post-treatment with IC_{50} of DOX and CUR for 24, 48 and 72 hours.

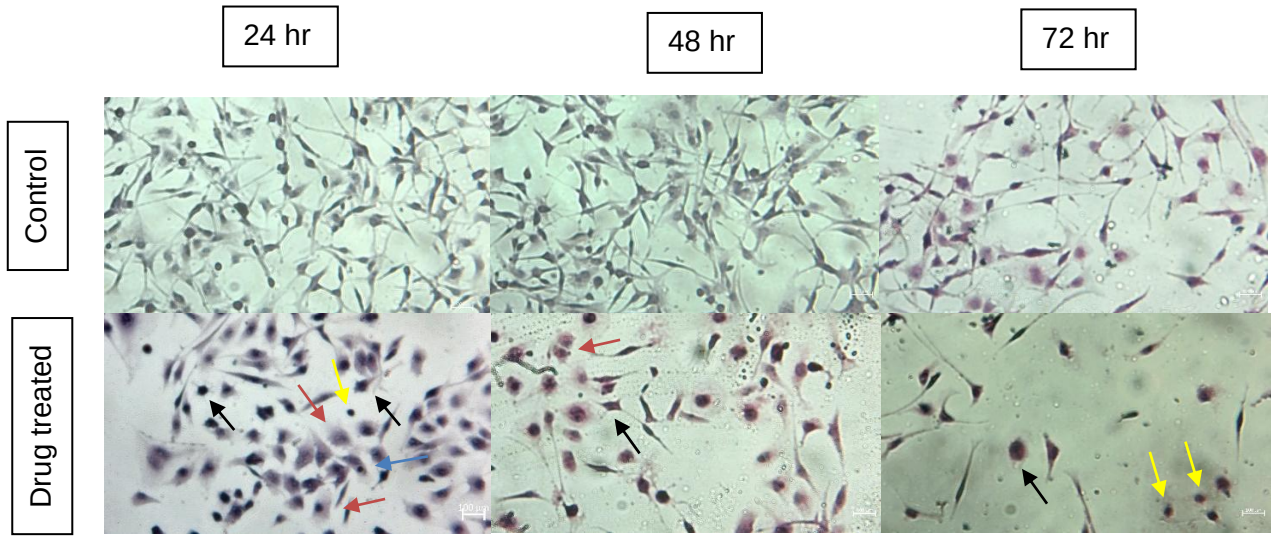

Note: Apoptotic features observed in treated cells are as follows: cell shrinkage (black arrows), membrane blebbing (red arrows), nuclear chromatin condensation (blue arrows) and apoptotic bodies formation (yellow). The images were captured at 200x magnification.

Figure 11

Hematoxylin & eosin (H&E staining) of MCF-7 control cells (top row) and treated cells (bottom row) post-treatment with IC_{50} of DOX and CUR for 24, 48 and 72 hours.

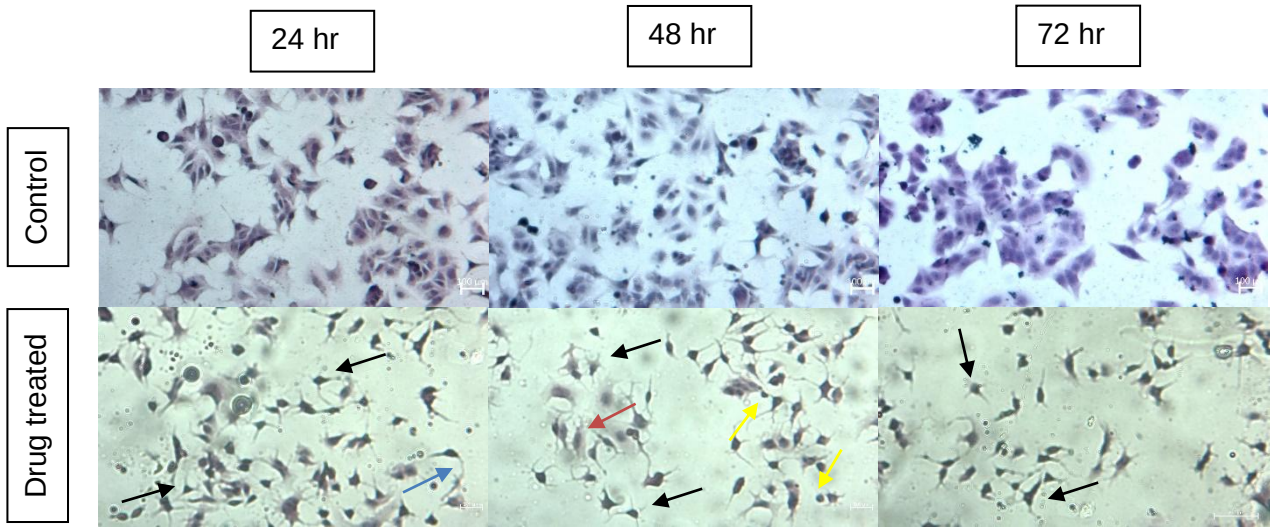

Note: Apoptotic features observed in treated cells are as follows: cytoplasmic shrinkage (black arrows), membrane blebbing (red arrows), apoptotic bodies formation (yellow arrows) and cytoplasmic extension (blue arrows). The images were captured at 200x magnification.

RT-PCR of *CDH1*

As aforementioned, *CDH1* expression level was quantified by comparing the gel electrophoresis band intensity of *CDH1* to that of *β-actin*, with *β-actin* normalised to an expression level of 1. Through analysis and calculation of expression levels, it can be observed that *CDH1* expression levels were more prominent in MDA-MB-231 treated cells with an expression level of 3.255 (Figure 12 and 13). However, MCF-7 treated cells had a decreased expression level of *CDH1* of 0.559 as compared to MCF-7 control cells.

Figure 12

Representative gel electrophoresis of duplicates from one independent experiment for untreated and treated MDA-MB-231 and MCF-7 cells with IC_{50} of DOX and CUR expressing CDH1 (93 bp), with β-actin (184 bp) as the housekeeping gene.

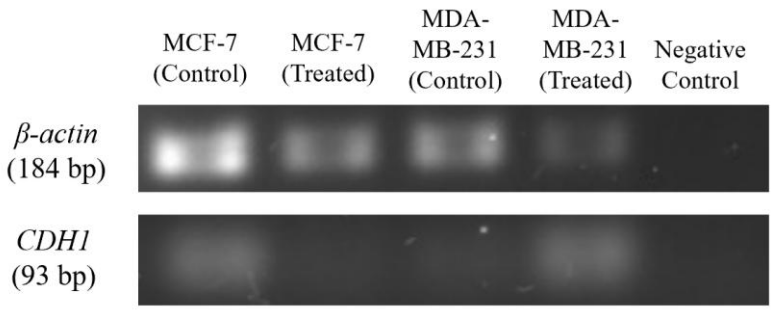

Note: CDH1: E-cadherin gene; β-actin: Beta-globin gene

Figure 13

Expression levels of CDH1 in untreated and treated MDA-MB-231 and MCF-7 cells 24 hours post-treatment with IC_{50} of DOX and CUR.

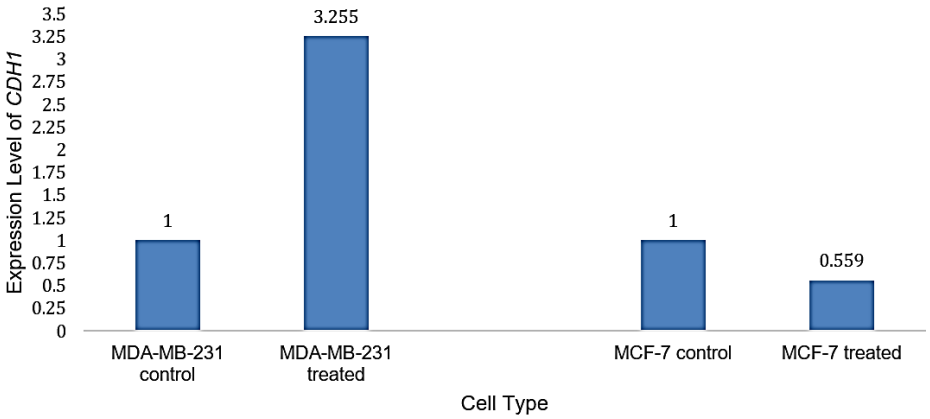

Note: Expression level of CDH1 was determined by measuring band intensities using ImageJ, normalized to β-actin, with the control set to 1 and treated samples expressed relative to the control.

DISCUSSION

Despite tremendous advancements in cancer therapy which has improved the prognosis of breast cancer patients over the past few decades, TNBC remains the subtype with the poorest prognosis, and is a leading cause of breast cancer-related mortality. This is largely attributed to its aggressive nature and limited response to currently available treatments (Almansour, 2022). The average survival time for patients with TNBC is approximately 10.2 months. Therefore, continued research is imperative to develop effective strategies to combat this highly aggressive disease.

Recent studies have highlighted the potential of CUR as an anticancer adjuvant, capable of suppressing cancer cell proliferation and reducing the development of chemoresistance. In this study, the established chemotherapeutic drug DOX was combined with CUR to study their anticancer effects in breast cancer cell lines.

At the IC_{50} of the combined treatment (0.8 µM of DOX and 20 µM of CUR), both MDA-MB-231 and MCF-7 cells displayed decreasing cell viability in a concentration-dependent manner. Based on our previous study, either the single treatment of DOX and CUR is more cytotoxic towards the TNBC cells like MDA-MB-231 than MCF-7 and the normal human breast epithelial cells MCF10A (Kong et al., 2019). At 24 hours post-treatment, MDA-MB-231 cells treated with single treatment of DOX (0.8 µM) and of CUR (20 µM) at their respective IC_{50} values showed significant reductions in viability to 57.82% ($p<0.05$) and 48.88% ($p<0.01$), respectively (Kong et al., 2019). The combined treatment of DOX and CUR at the same concentrations in this study further reduced the viability to 54% very significantly ($p< 0.001$), compared to DOX treatment alone as aforementioned. A study conducted by Rashmi et al. (2020), has shown similar findings where CUR displayed concentration-dependent cytotoxicity in MDA-MB-231, resulting in a IC_{50} of 18.54 µM. Although Wang et al. (2020) found that DOX had an IC_{50} of 1.65 µM ± 0.23, this differs with the resulting IC_{50} of 0.8 µM, which can be explained by CUR's presence thus, combinatory ability to reduce the IC_{50} value of DOX (Wen et al., 2019).

MTT assay revealed a time-dependent decrease in cell viability for both breast cancer cell lines treated with combined DOX and CUR, with MDA-MB-231 showing a significant steady decline ($p < 0.001$). Similar findings were reported by Klippstein et Al. (2016), where DOX and CUR combination increased apoptosis and reduced viability in prostate cancer cells. This combination also enhanced apoptosis in M5076 ovarian sarcoma cells via caspase-independent pathway and apoptosis-inducing factor (Sadzuka et al., 2012). Additionally, enhanced sensitivity in MCF-7 and MDA-MB-231 cells was reported when DOX was combined with CUR and curcumol (another natural bioactive compound), respectively (Meiyanto et al., 2014; Zeng et al., 2020). These results show how CUR, and its analogues are effective in induction of cell apoptosis and inhibition of NF-κB which is responsible for cell survival.

DOX is known to induce apoptosis by inhibiting drug efflux pumps such as ATP-binding cassette (ABC) transporters, notably ABCC3, ABCB1 and ABCB4, thereby reducing chemoresistance and improving efficacy in reducing cell viability (Zeng et al., 2020). This mechanism may explain the consistently low cell viability observed for MDA-MB-231 between 48 and 72 hours post-treatment results as drug efflux inhibition prolongs drug activity.

For MCF-7 cells, the uptick at 48 hours post-treatment may indicate emerging DOX resistance, potentially driven by increased expression of multidrug resistance proteins such as NF-κB, MDR1, and CD44, which alter drug pharmacokinetics (Fang et al., 2014). Additionally, elevated ABC transporter activity could contribute to chemoresistance by promoting drug efflux (Farghadani and Naidu, 2022).

Trypan blue exclusion confirmed a significant decrease in viability for both cell lines. MCF-7 showed a more gradual decline compared to MDA-MB-231. This was expected, as ERα-positive MCF-7 cells are less sensitive to DOX (Wan et al., 2021). Nonetheless, reductions in MCF-7 viability were significant at all time points. Furthermore, MCF-7 cells exhibited the lowest cell viability at the 72 hours timepoint, as compared to MDA-MB-231 cells. It is likely that due to prolonged treatment of DOX and CUR in MCF-7 cells for 72 hours, the MCF-7 cells grew susceptible to the combined treatment of DOX and CUR. This is plausible, as MCF-7 cells are of the luminal A subtype and have low expression levels of the Ki-67 cell proliferation marker protein (Yuan et al., 2016). The expression levels of Ki-67 have been found to be correlated with the pathogenesis of breast cancer. This results in the slower growth rates of MCF-7 cell lines, making them more susceptible to treatment, as they are less aggressive than TNBC subtypes.

A very significant and sharp decrease in cell viability was observed in MDA-MB-231 cells at all timepoints. However, a slight (1%) increase in cell viability was observed at the 72 hours timepoint, although this is not statistically significant. However, this could still be suggestive of chemoresistance in MDA-MB-231 cells due to the aggressive and heterogenous nature of TNBC cells (Ozcelikkale et al., 2017), as well as their higher tendency to express more epithelial growth factor receptor (EGFR) compared to other breast cancer subtypes (Obidiro et al., 2023).The phenomena of cancer cell repopulation could also explain the increase in cell viability of MDA-MB-231 cells, whereby the rapid proliferation of a surviving population of cancer cells occurs after chemotherapy-induced cell killing (Prakash & Telleria, 2023).

Nevertheless, both cell lines showed a significant decline in viability compared to controls, consistent with previous findings that DOX and CUR combination enhanced the chemosensitivity. CUR as an adjuvant reduced the IC_{50} of DOX by approximately two-fold (Zhou et al., 2015). This is supported by another study that the intracellular accumulation of DOX increased when cells were co-treated with CUR (Wen et al., 2019). The profound effects of CUR were further proven in TNBC cells. CUR was found to suppress the acquisition of epithelial-mesenchymal transition (EMT), which resulted in the prevention of multi-drug resistance (Chen et al., 2013). CUR also was found to enhance the effects of DOX-induced apoptosis. Furthermore, the effect of CUR as a chemotherapeutic adjuvant has also been found to inhibit the self-renewal capacity of breast cancer stem cells, which are a major contributor that confers chemoresistance to cancer cells (Zhou et al., 2015). Therefore, the ability to target the stem cell population suggests the ability to effectively eliminate a cancer cell population whilst successfully mitigating drug resistance in cancers.

The wound healing assay was performed where it mimics directional cell migration *in vivo* through creating an artificial wound in the cell monolayer and observing the beginning and in regular timed intervals to observe wound closure and quantifying the rate of migration. This can in turn be used to evaluate the anti-metastasis effect of the potential therapeutic drug.

The findings show that MDA-MB-231 cells treated with combinatory DOX and CUR had successfully inhibited cell migration after 72 hours post-treatment when compared to the 0-hour timepoint, though it was not statistically significant. As MDA-MB-231, a TNBC, is notorious for its highly aggressive, invasive and migratory nature, it explains that the combined treatment is only effective after longer incubation. Through compelling evidence, this antimigratory effect can be explained by decreased EMT, featuring an upregulation of E-cadherin (*CDH1*), thus leading to reduced migration and invasion characteristics of cancer cells (Chen et al., 2013). This favourable drug induced effect can be caused by the combination treatment, where DOX has been studied to present undesirable malignant features through increased EMT and drug resistance, Chen et al. shows CUR's ability to reverse and inhibit DOX induced EMT, through inhibiting TGF-β and PI3K/AKT signalling pathways (Chen et al., 2013). Where EMT contributes to cancer metastasis, this combination treatment proves to be useful to treat TNBC.

In MCF-7 cells, the combination treatment effectively inhibited migration at the 24 and 48 hours, likely due to CUR's ability to suppress NF-κB pathway activation, thereby reducing downstream gene expression involved in invasion and metastasis. Migration and invasion are driven by activation of MMPs, which degrade the extracellular matrix to facilitate

invasion. The increased migration observed at 72 hours may be attributed to PI3K-dependent activation of Akt and NF-κB in MCF-7, promoting resistance to chemotherapeutic agents such as DOX (Chen et al., 2013).

However, some reduction in wound closure in untreated cells may reflect differences in proliferation rather than migration, potentially skewing relative wound closure measurements. The trans-well migration assay could serve as a quantitative alternative to study cell migration, mitigating lack of standardization from the wound healing assay as supported by Chen (2012) using MDA-MB-231 cells. Nonetheless, the efficacy of the combination treatment of this study highlights its potential to inhibit metastasis of the aggressive breast cancer cells.

Cell viability results were further supported by morphological observations and H&E staining. The cytotoxic effects of the anticancer agents can be confirmed through morphological observation, and H&E staining offers a simple, cost-effective method for detecting apoptotic cells (Roudsari et al., 2012; Nayak et al., 2016). Both MDA-MB-231 and MCF-7 exhibited apoptotic features including cell shrinkage, membrane blebbing, and apoptotic body formation along with nuclear chromatin condensation in MDA-MB-231 and cytoplasmic extension in MCF-7, compared to the untreated cells. These findings confirm that the DOX and CUR combination induced apoptosis. Our previous study has demonstrated that MDA-MB-231 cells treated with single DOX (0.8 µM) and single CUR (20 µM) at their respective IC_{50} at 24, 48 and 72 hours post-treatment exhibited apoptotic features including cell shrinkage and nuclear chromatin condensation (Kong, 2019). These apoptotic features were minimally observed in MCF10A under the same treatments and these results were validated through cleavage of PARP in Western blotting analysis (Kong et al., 2019). In addition, for more accurate viability assessment, complementary assays such as the ATP-based tests, which are rapid, sensitive and evaluate both cell viability and apoptosis through membrane integrity, could be employed (Riss et al., 2004).

Cancer metastasis and progression are often associated with EMT, characterized by loss of cell adhesion and increased mobility, typically accompanied by reduced *CDH1* expression. In this study, MDA-MB-231 cells showed elevated *CDH1* levels following combination treatment, suggesting successful EMT inhibition and reduced metastatic potential (Kewitz, 2013). This aligns with findings by Chen et al (2013), where CUR suppressed EMT and DOX induced *CDH1* expression via PI3K/Akt pathway inhibition, enhancing antiproliferative effects in TNBC cells. Conversely, the treated MCF-7 cells exhibited reduced *CDH1* expression, indicated limited efficacy in preventing invasion and metastasis, consistent with previous reports where CUR failed to enhance E-cadherin expression in ER-positive cells (Ziegler et al., 2014; Paramita et al., 2018). To further validate the research findings obtained, Western blotting could be conducted to target E-cadherin protein expression, as mRNA and protein levels can be inconsistent, with transcriptomic changes not always corresponding to protein level changes (San et al., 2025). Nevertheless, the research findings obtained from this study support the greater sensitivity of MDA-MB-231 to DOX in combination with CUR therapy.

CONCLUSION

Breast cancer remains a complex and life-threatening disease, with current therapies often limited by adverse effects. Combination treatments offer a promising strategy to overcome these challenges. DOX and CUR demonstrated great combinatory potential, effectively reducing cell proliferation, inhibiting migration, and inducing apoptosis. CUR contributed by suppressing EMT-related pathways and enhancing DOX's apoptotic effects, likely through upregulation of E-cadherin (*CDH1*). Additionally, CUR may mitigate DOX-associated toxicity while targeting multiple signalling pathways, reinforcing its role as an effective adjuvant. These findings highlight the therapeutic promise of the combination treatment of DOX and CUR and warrant further research, optimization, and clinical evaluation as a novel approach to improve breast cancer treatment outcomes.

AUTHOR CONTRIBUTIONS

Yee Teng Wong and Ashley San Ann Soo were responsible for the acquisition and analysis of data, as well as manuscript writing. Ser Hui San was responsible to provide guidance throughout the project, assisted in troubleshooting experimental issues, analysis and interpretation of results. Siew Ching Ngai as the supervisor, contributed to the conception and design of the study, provided supervision throughout the project, as well as critically revised the manuscript and improved the clarity and quality of the manuscript.

ETHICS APPROVAL

Not applicable.

FUNDING

Not applicable.

CONFLICT OF INTEREST

The authors declare no conflict of interest in this work.

ACKNOWLEDGEMENT

The authors would like to acknowledge the University of Nottingham Malaysia for providing the resources for this Final Year Research Project for the Bachelor of Science (Honours) in Biotechnology.

REFERENCES

Almansour, N.M. (2022). Triple-negative breast cancer: A brief review about epidemiology, risk factors, signaling pathways, treatment and role of artificial intelligence. *Frontiers in Molecular Biosciences, 9*: 836417. https://doi.org/10.3389/fmolb.2022.836417

Chen, Y. (2012). Transwell Cell Migration Assay Using Human Breast Epithelial Cancer Cell. Bio-protocol, 2(4): e99. https://doi.org/10.21769/BioProtoc.99

Chen, W.-C., Lai, Y.-A., Lin, Y.-C., Ma, J.-W., Huang, L.-F., Yang, N.-S., Ho, C.-T., Kuo, S.-C. & Way, T.-D. (2013). Curcumin suppresses doxorubicin-induced epithelial–mesenchymal transition via the inhibition of TGF-β and PI3K/AKT signaling pathways in triple-negative breast cancer cells. *Journal of Agricultural and Food Chemistry, 61*(48): 11817–11824. https://doi.org/10.1021/jf404092f

Fang, X.J., Jiang, H., Zhu, Y.Q., Zhang, L. Y., Fan, Q.H., & Tian, Y. (2014). Doxorubicin induces drug resistance and expression of the novel CD44st via NF-κB in human breast cancer MCF-7 cells. *Oncology Reports, 31*(6): 2735–2742. https://doi.org/10.3892/or.2014.3131

Farghadani, R. & Naidu, R. (2022). Curcumin as an enhancer of therapeutic efficiency of chemotherapy drugs in breast cancer. *International Journal of Molecular Sciences, 23*(4): 2144. https://doi.org/10.3390/ijms23042144

Feitelson, M.A., Arzumanyan, A., Kulathinal, R.J., Blain S.W., Holcombe, R.F., Mahajna, J., Marino, M., Martinez-Chantar, M.L., Nawroth, R., Sanchez-Garcia, I., Sharma, D., Saxena, N.K., Singh, N., Vlachostergios, P.J., Guo, S., Honoki, K., Fujii, H., Georgakilas, A.G., Bilsland, A., Amedei, A., Niccolai, E., Amin, A., Ashraf, S.S., Boosani, C.S., Guha, G., Ciriolo, M.R., Aquilano, K., Chen, S., Mohammed, S.I., Azmi, A.S., Bhakta, D., Halicka, D., Keith, W.N. & Nowsheen, S. (2015). Sustained proliferation in cancer: Mechanisms and novel therapeutic targets. *Seminars in Cancer Biology, 35*: S25–S54. https://doi.org/10.1016/j.semcancer.2015.02.006

Iacopetta, D., Ceramella, J., Baldino, N., Sinicropi, M.S. & Catalano, A. (2023). Targeting breast cancer: An overlook on current strategies. *International Journal of Molecular Sciences, 24*(4): 3643. https://doi.org/10.3390/ijms24043643

Jalaladdiny, S., Badoei-dalfard, A, Karami, Z. & Sargazi. G. (2022). Co-delivery of doxorubicin and curcumin to breast cancer cells by a targeted delivery system based on Ni/Ta core-shell metal-organic framework coated with folic acid-activated chitosan nanoparticle. *Journal of the Iranian Chemical Society, 19*(10): 4287–4298. https://doi.org/10.1007/s13738-022-02604-w

Jin, S., Yang, Y., Ma, L., Ma, B., Ren, L., Guo, L., Wang, W., Zhang, Y., Zhao, Z. & Cui, M. (2017). *In vivo* and *in vitro* induction of the apoptotic effects of oxysophoridine on colorectal cancer cells via the Bcl-2/Bax/caspase-3 signaling pathway. *Oncology Letters, 14*(6): 8000-8006. https://doi.org/10.3892/ol.2017.7227

Kewitz, S., Volkmer, I & Staege, M.S. (2013). Curcuma contra cancer? Curcumin and Hodgkin's lymphoma. *Cancer Growth Metastasis, 6:* 35-52. https://www.ncbi.nlm.nih.gov/pmc/articles/PMC3941149/

Klippstein, R., Bansal, S.S. & Al-Jamal, K.T. (2016). Doxorubicin enhances curcumin's cytotoxicity in human prostate cancer cells in vitro by enhancing its cellular uptake. *International Journal of Pharmaceutics, 514*(1): 169–175. https://doi.org/10.1016/j.ijpharm.2016.08.003

Kong, W. Y. (2019). Zebularine and trichostatin a sensitized human breast adenocarcinoma cells towards tumour necrosis-factor-related apoptosis inducing ligand (TRAIL)-induced apoptosis. MRes thesis, University of Nottingham. https://eprints.nottingham.ac.uk/id/eprint/56550

Kong, W. Y., Yee, Z.Y., Mai, C.W., Fang, C.-M., Abdullah, S. & Ngai, S.C. (2019). Zebularine and trichostatin A sensitized human breast adenocarcinoma cells towards tumor necrosis factor-related apoptosis inducing ligand (TRAIL)-induced apoptosis. *Heliyon 5*: e02468. https://doi.org/10.1016/j.heliyon.2019.e02468

Lee, M.-G., Lee, K.-S. & Nam, K.-S. (2023). Combined doxorubicin and arctigenin treatment induce cell cycle arrest-associated cell death by promoting doxorubicin uptake in doxorubicin-resistant breast cancer cells. *IUBMB Life, 75*(9): 765–777. https://doi.org/10.1002/iub.2772

Lim, S. W., Ting, K. N., Bradshaw, T. D., Zeenathul, N. A., Wiart, C., Khoo, T. J., Lim, K. H., & Loh, H. S. (2011). *Acalypha wilkesiana* extracts induce apoptosis by causing single strand and double strand DNA breaks. *Journal of Ethnopharmacology, 138*(2): 616–623. https://doi.org/10.1016/j.jep.2011.10.005

Lovitt, C. J., Shelper, T. B., & Avery, V. M. (2018). Doxorubicin resistance in breast cancer cells is mediated by extracellular matrix proteins. *BMC Cancer, 18*(1): 41. https://doi.org/10.1186/s12885-017-3953-6

Meiyanto, E., Putri, D.D.P., Susidarti, R.A., Murwanti, R., Sardjiman, Fitriasari, A., Husnaa, U., Purnomo, H. & Kawaichi, M. (2014). Curcumin and its analogues (PGV-0 and PGV-1) enhance sensitivity of resistant MCF-7 cells to doxorubicin through inhibition of HER2 and NF-kB activation. *Asian Pacific Journal of Cancer Prevention, 15*(1): 179-84. https://doi.org/10.7314/apjcp.2014.15.1.179

Nayak, A., Raikar, A., Kotrashetti, V., Nayak, R., Shree, S. & Kambali, S. (2016). Histochemical detection and comparison of apoptotic cells in the gingival epithelium using hematoxylin and eosin and methyl green-pyronin. *Journal of Indian Society of Periodontology 20*(3): 394-298. https://doi.org/10.4103/0972-124x.182601

Obidiro, O., Battogtokh, G., & Akala, E. O. (2023). Triple Negative Breast Cancer Treatment Options and Limitations: Future Outlook. *Pharmaceutics, 15*(7): 1796. https://doi.org/10.3390/pharmaceutics15071796

Ozcelikkale, A., Shin, K., Noe-Kim, V., Elzey, B. D., Dong, Z., Zhang, J.-T., Kim, K., Kwon, I. C., Park, K., & Han, B. (2017). Differential response to doxorubicin in breast cancer subtypes simulated by a microfluidic tumor model. *Journal of Controlled Release*, *266*: 129–139. https://doi.org/10.1016/j.jconrel.2017.09.024

Paramita, P., Wardhani, B.W.K., Wanandi, S.I. & Louisa, M. (2018). Curcumin for the Prevention of Epithelial-Mesenchymal Transition in Endoxifen-Treated MCF-7 Breast Cancer Cells. *Asian Pacific Journal of Cancer Prevention 19*(5): 1243–1249. https://doi.org/10.22034/APJCP.2018.19.5.1243

Pilco-Ferreto, N., & Calaf, G. M. (2016). Influence of doxorubicin on apoptosis and oxidative stress in breast cancer cell lines. International *Journal of Oncology, 49*(2): 753–762. https://doi.org/10.3892/ijo.2016.3558

Prakash, R., & Telleria, C. M. (2023). Cancer cell repopulation after therapy: which is the mechanism? *Oncoscience, 10*: 14–19. https://doi.org/10.18632/oncoscience.577

Pulido-Moran, M., Moreno-Fernandez, J., Ramirez-Tortosa, C & Ramirez-Tortosa, M. (2016). Curcumin and Health. *Molecules, 21*(3): 264. https://doi.org/10.3390/molecules21030264

Rashmi, R., Prakash, N., Naravanaswamy, H., Swamy, M., Rathnamma, D., Ramesh, P., Sunilchandra, U., Naveenkumar, S. Kumar, K. & Vanishree, H. (2020). Evaluation of curcumin for cytotoxicity potential on MDA-MB-231 cancer cell lines. *Journal of Entomology and Zoology Studies, 8*(1): 270-272. https://www.academia.edu/127289656/Evaluation_of_curcumin_for_cytotoxicity_potential_on_MDA_MB_231_cancer_cell_lines

Riss, T. L., Moravec, R.A., Niles, A.L., Duellman, S, Benink, H.A., Worzella, T.J. & Minor, L. (2004). Assay Guidance Manual. Eli Lilly & Company and the National Center for Advancing Translational Sciences. http://www.ncbi.nlm.nih.gov/books/NBK144065/

Roudsari, M. T., Bahrami, A.R., Dehghani, H., Iranshahi, M., Matin, M.M. & Mahmoudi, M. (2012). Bracken-fern extracts induce cell cycle arrest and apoptosis in certain cancer cell lines. *Asian Pacific Journal of Cancer Prevention 13*(12): 6047-6053. http://dx.doi.org/10.7314/APJCP.2012.13.12.6047

Rodriguez, L.G., Wu, X. and Guan, J.-L. (2005) 'Wound-Healing Assay', in J.-L. Guan (ed.) Cell Migration: Developmental Methods and Protocols. Totowa, NJ: Humana Press (Methods in Molecular Biology™), pp. 23–29. https://doi.org/10.1385/1-59259-860-9:023

Sadzuka, Y., Nagamine, M., Toyooka, T., Ibuki, Y. & Sonobe, T. (2012). Beneficial effects of curcumin on antitumor activity and adverse reactions of doxorubicin. *International Journal of Pharmaceutics, 432*(1): pp. 42–49. https://doi.org/10.1016/j.ijpharm.2012.04.062

Saharkhiz, S., Zarepour, A. Nasri, N. Cordani, M & Zarrabi, A. (2023). A comparison study between doxorubicin and curcumin co-administration and co-loading in a smart niosomal formulation for MCF-7 breast cancer therapy. *European Journal of Pharmaceutical Sciences, 191*: 106600. https://doi.org/10.1016/j.ejps.2023.106600

San, S.H., Wong, S.H.M., Fang, C.-M., Ngai, S.C. (2025). Elucidating the potential of E-cadherin re-expression along with Trichostatin A and Zebularine in enhancing Tumour necrosis factor-related apoptosis-inducing ligand (TRAIL)-induced apoptosis in human breast adenocarcinoma cells.

San, S.H. & Ngai, S.C. (2025). The synergistic anticancer effects of curcumin in combination with breast cancer chemotherapy drugs. Life Sciences, Medicine and Biomedicine, 9(1): 173. https://doi.org/10.28916/lsmb.9.1.2025.173

Current Cancer Drug Targets. (In Press) https://doi.org/10.2174/0115680096374361250610075556

Sheikholeslami, A., Nabiuni, M. and Arefian, E. (2017). Suppressing the molecular signaling pathways involved in inflammation and cancer in breast cancer cell lines MDA-MB-231 and MCF-7 by miR-590. *Tumor Biology, 39*(4). https://doi.org/10.1177/1010428317697570

Song, X., Zhang, M., Dai, E. & Luo, Y. (2019). Molecular targets of curcumin in breast cancer (Review). *Molecular Medicine Reports, 19*(1): 23–29. https://doi.org/10.3892/mmr.2018.9665

Strober, W. (2015). Trypan blue exclusion test of cell viability. *Current Protocols in Immunology, 111*(1). https://doi.org/10.1002/0471142735.ima03bs111

Wan, X., Hou, J., Liu, S., Zhang, Y., Li, W., Zhang, Y & Ding, Y. (2021). Estrogen receptor α mediates doxorubicin sensitivity in breast cancer cells by regulating E-Cadherin. *Frontiers in Cell and Developmental Biology, 9*: 583572. https://doi.org/10.3389/fcell.2021.583572

Wang, F., Xiang, Z., Huang, T., Zhang. M. & Zhou, W.B. (2020). ANLN Directly Interacts with RhoA to promote doxorubicin resistance in breast cancer cells. *Cancer Management and Research, 12*: 9725–9734. https://doi.org/10.2147/CMAR.S261828

Wen, C., Fu, L., Huang, J., Dai, Y., Wang, B., Xu, G., Wu, L. & Zhou, H. (2019). Curcumin reverses doxorubicin resistance via inhibition the efflux function of ABCB4 in doxorubicin-resistant breast cancer cells. *Molecular Medicine Reports, 19*(6): 5162–5168. https://doi.org/10.3892/mmr.2019.10180

Wong, S.H.M., Fang, C.-M., Loh, H.-S. & Ngai, S.C. (2021). Trichostatin A and zebularine along with E-cadherin re-expression enhance tumour necrosis factor-related apoptosis-inducing ligand (TRAIL)-mediated cell cycle arrest in human breast adenocarcinoma cells. *Asia-pacific Journal of Molecular Biology and Biotechnology*, *29*(1):26–41. https://doi.org/10.35118/apjmbb.2021.029.1.04

World Health Organization (2024) Breast cancer. https://www.who.int/news-room/fact-sheets/detail/breast-cancer (Accessed: 27 April 2024).

Xia, Y., Shen, S. and Verma, I.M. (2014). NF-κB, an active player in human cancers. *Cancer Immunology Research, 2*(9): 823–830. https://doi.org/10.1158/2326-6066.CIR-14-0112.

Yap, Z.H., Kong, W. Y., Azeez, A.R., Fang, C.-M. & Ngai, S.C. (2022). Anti-cancer effects of epigenetics drugs scriptaid and zebularine in human breast adenocarcinoma cells. *Anti-Cancer Agents in Medicinal Chemistry, 22*(8): 1582–1591. https://doi.org/10.2174/1871520621666210608103251

Yuan, L., Cai, Y., Zhang, L., Liu, S., Li, P. & Li, X. (2022). Promoting apoptosis, a promising way to treat breast cancer with natural products: A comprehensive review. *Frontiers in Pharmacology, 12*. https://doi.org/10.3389/fphar.2021.801662

Yuan, P., Xu, B., Wang, C., Zhang, C., Sun, M. & Yuan, L. (2016). Ki-67 expression in luminal type breast cancer and its association with the clinicopathology of the cancer. *Oncology Letters, 11*(3): 2101–2105. https://doi.org/10.3892/ol.2016.4199

Zeng, C., Fan, D., Xu, Y., Li, X., Yuan, J., Yang, Q., Zhou, X., Lu, J., Zhang, C., Han, J., Gu, J., Gao, Y., Sun, L. & Wang, S. (2020). Curcumol enhances the sensitivity of doxorubicin in triple-negative breast cancer via regulating the miR-181b-2-3p-ABCC3 axis. *Biochemical Pharmacology, 174*: 113795. https://doi.org/10.1016/j.bcp.2020.113795

Zhou, Q., Ye, M., Lu, Y., Zhang, H., Chen, Q., Huang, S. & Su, S. (2015). Curcumin improves the tumoricidal effect of mitomycin C by suppressing ABCG2 expression in stem cell-like breast cancer cells. *PLOS ONE, 10*(8): e0136694. https://doi.org/10.1371/journal.pone.0136694

Ziegler, E., Hansen, M.-T., Haase, M., Emons, G. & Gründker, C. (2014). Generation of MCF-7 cells with aggressive metastatic potential in vitro and in vivo. *Breast Cancer Research and Treatment, 148*(2): 269–277. https://doi.org/10.1007/s10549-014-3159-4

Citation:

Wong, Y. T., Soo, A. S. A., San, S. H., & Ngai, S. C. (2026). Anticancer combination effects of Doxorubicin and Curcumin on human breast cancer cell lines MDA-MB-231 and MCF-7. *Life Sciences, Medicine and Biomedicine*, *10*(1). https://doi.org/10.28916/lsmb.10.1.2026.177

Life Sciences, Medicine and Biomedicine
ISSN: 2600-7207

Copyright © 2026 by the Author(s). Life Sciences, Medicine and Biomedicine (ISSN: 2600-7207) Published by Biome Journals - Biome Scientia Sdn. Bhd. Attribution 4.0 International (CC BY 4.0). This open access article is distributed based on the terms and conditions of the Creative Commons Attribution license https://creativecommons.org/licenses/by/4.0/